Specific heat of $YBa_2Cu_3O_{7-\delta}$

Kathryn A. Moler,* David L. Sisson, Jeffrey S. Urbach,† Malcolm R. Beasley, and Aharon Kapitulnik
Departments of Physics and Applied Physics, Stanford University, Stanford, California 94305

David J. Baar, Ruixing Liang, and Walter N. Hardy
Department of Physics, University of British Columbia, Vancouver, British Columbia, Canada V6T1Z1

(Received 14 May 1996)

We present measurements of the specific heat of $YBa_2Cu_3O_{7-\delta}$ single crystals from 2 to 10 K and from 0 to 10 T, including both twinned and untwinned crystals with various oxygen doping ($7-\delta=6.95$, 6.97, and 6.99). The zero-field specific heat includes a linear-T term which is small compared to other $YBa_2Cu_3O_{7-\delta}$ samples, but large compared to the T^2 electronic specific heat predicted for a superconductor with clean lines of nodes in the gap function. This zero-field linear-T term is found to decrease with decreasing concentration of twin boundaries and oxygen vacancies δ. The specific heat increases in a magnetic field and has a strong dependence on field orientation. Several possible field-dependent contributions are compared to the data, including a Schottky anomaly, vortex-vortex interactions, a traditional mixed-state HT term associated with vortex cores, and a $\sqrt{H}T$ term predicted by G. Volovik for the mixed state in superconductors with lines of nodes in the gap function. The field dependence of the specific heat, according to a comparison of fits based on these possibilities, supports the existence of lines of nodes and suggests the presence of quasiparticle excitations outside the vortex core. [S0163-1829(96)08146-5]

I. INTRODUCTION

In conventional BCS superconductors, the absence of low-energy electronic excitations is reflected in the thermodynamic properties such as the specific heat, c. The theoretical electronic specific heat is proportional to $e^{-\Delta_0/k_BT}$, where Δ_0 is the energy gap.[1] Although small deviations from exponential behavior have been observed in some materials at the lowest temperatures,[2] the specific heat of most conventional superconductors is experimentally found to be exponential at low temperatures.[3,4] In contrast, if the gap is zero somewhere on the Fermi surface, that is, if the gap has nodes, then the thermodynamic properties will decrease as some power of the temperature which is determined by the nature of the nodes. For example, the quasi-two-dimensional d-wave gap function proposed for cuprate superconductors has a low-energy density of states which obeys $N(E)\propto|E-E_F|$, and the theoretical low-temperature electronic specific heat obeys $c=\alpha T^2$.

A variety of experiments related to the symmetry of the order parameter and to the structure of the density of states in cuprate superconductors are reviewed in Refs. 5 and 6. The low-energy excitations are probed by penetration depth,[7,8] NMR,[9] photoemission,[10] specific heat,[11] and Raman scattering,[12] while a number of ingenious Josephson junction schemes directly probe the symmetry of the gap.[13–17] In particular, measurements on $YBa_2Cu_3O_{7-\delta}$ single crystals show a linear temperature dependence of the microwave penetration depth,[7,8] as predicted for superconductors with lines of nodes in the clean limit.[18]

All measurements of the low-temperature specific heat on cuprate superconductors have shown the presence of low-energy excitations.[19,20] Samples of $YBa_2Cu_3O_{7-\delta}$ generally have a γT term with a coefficient $\gamma\geqslant 4$ mJ/mol K^2, which is a significant fraction of the literature values for the normal-state density of states, $\gamma_n\simeq 20$ mJ/mol K^2.[20,21] The analyses of these data are complicated: the specific heat contains information about *all* excitations, low-temperature specific heat curves are typically smooth and featureless, and physically motivated fitting functions contain many free parameters. The coefficient α of any quadratic term associated with clean lines of nodes may be theoretically estimated from the slope of the density of states as $\alpha\approx\gamma_n T(T/T_c)$. More exact estimates require knowledge of such factors as the ratio $\Delta_{\max}/kT_c$ and the angular dependence of the normal-state density of states, N_n.[22–24] Because this estimated αT^2 term is less than or comparable to 5% of the phonon specific heat at 2 K, most measurements neither rule out nor confirm the existence of this term.

We have previously reported on the specific heat of YBCO single crystals similar to those which show a linear-T temperature dependence of the penetration depth.[11,25] These measurements and analysis showed a $\sqrt{H}T$ term, predicted by Volovik for superconductors with lines of nodes,[26] and an αT^2 term. Both terms agreed semiquantitatively with the theoretical predictions for lines of nodes.[22–24,26] The specific heat data also showed a zero-field linear-T term, which is inconsistent with clean lines of nodes if it is associated with the superconducting electrons.

This paper has two main purposes. First, we present a more extensive discussion of the possible contributions to the specific heat than we have presented elsewhere. Models for these contributions are discussed in Sec. V and include phonons and zero-field electronic excitations, as well as several possible field-dependent excitations: a Schottky anomaly (which may be anisotropic), a Debye-like specific heat resulting from vortex-vortex interactions, a traditional high-κ mixed-state HT term associated with vortex cores, and a $\sqrt{H}T$ term predicted by Volovik for the mixed state in su-

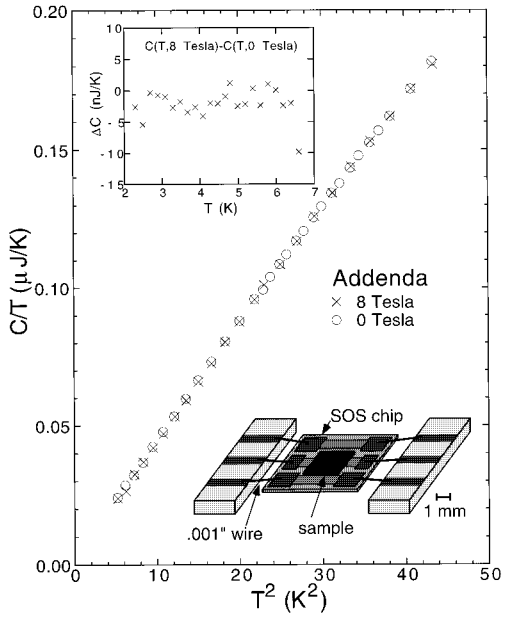

FIG. 1. Measured addenda heat capacity at 0 and 8 T, plotted as C/T vs T^2. Bottom right inset: schematic of a sample mounted on a silicon-on-sapphire chip. Upper left inset: difference between the measured addenda heat capacity at 8 and 0 T.

perconductors with lines of nodes in the gap function.[26] Secondly, we report additional measurements on the dependence of the specific heat on twins and on oxygenation, with oxygen doping levels of $7-\delta=6.95$, 6.97, and 6.99. These measurements show that the zero-field linear-T term decreases significantly with decreasing concentrations of twins and oxygen vacancies. The Schottky anomaly and the T^3 term also decrease with decreasing δ.

II. TECHNIQUE

All heat capacity measurements share the common feature that a sample (heat capacity C_s) together with some addenda (heat capacity C_{add}) are coupled to a thermal bath via a thermal link κ_w. The heat capacity data presented here were taken with the relaxation method,[27] in which the heat capacity is determined by a direct measurement of the thermal time constant, $\tau=(C_s+C_{\text{add}})/\kappa_w$. In contrast to adiabatic calorimetry, the relaxation method puts less stringent requirements on the thermal isolation of the sample and allows a smaller sample size.

The sample is attached with a small amount of Wakefield thermal compound ($\sim 10\ \mu$g) to a sapphire chip. Each chip has a thin-film heater and two thermometers made of phosphorus-doped silicon with aluminum contact pads.[28] The silicon-on-sapphire (SOS) chip is suspended from a copper block by 0.001 in. Au-7% Cu wires [Fig. 1 (inset)]. The relaxation time τ is measured by heating the SOS chip to a temperature which is some tens of mK above the block temperature, cutting the power to the SOS chip heater, and observing the decay of the SOS chip temperature back to the bath temperature. The relaxation is well-described by a single exponential throughout the measurement range, confirming that there is only a single slow time constant, ranging from 5 milliseconds for small samples and low temperatures to 10 seconds for large samples and high temperatures. If the sapphire chip and the sample were not in thermal equilibrium with each other on this time scale, the relaxation would have a more complicated time dependence.

The thermal conductance of the gold wires, κ_w, depends on magnetic field and temperature. κ_w may also be changed by a few percent if there is a small physical shift in the position of the wires as a consequence of vibrations or magnetic-field-induced torques. Accordingly, κ_w is measured at each temperature and field during each run by applying a fixed power and measuring the resulting increase in the temperature of the sapphire chip, typically a few hundred mK. Since κ_w is approximately linear in T, this procedure corresponds to a measurement of κ_w at the midpoint of the block and sample temperature.

The SOS chip temperature is controlled and measured by the thin film heater and thermometers deposited directly onto the chip. The resistance of the SOS thermometer is monitored by a homemade computer programmable ac bridge run at a few kHz. A separate heater and calibrated carbon glass resistor (CGR) thermometer are used to control the temperature of the copper block, which is suspended in vacuum and is surrounded by an isothermal copper shield.

The data-taking program has been designed to be insensitive to the calibration of the thermometer on the SOS chip, essentially by using the cgr thermometer for a point-by-point calibration of the chip thermometer during a run.[25,29] Although cumbersome, this procedure compensates for the silicon thermometers' high magnetoresistance, chip-to-chip variation, and sensitivity to thermal cycling.

The measurements of τ are at different temperatures than the measurements of κ_w. Generally polynomial fits of up to third order have been used to interpolate the thermal conductance data. However, the data points are sufficiently dense and the scatter is sufficiently low that linear interpolations give an indistinguishable result. These interpolated thermal conductance values are combined with the relaxation times to determine the total heat capacity, $C_s+C_{\text{add}}=\kappa_w\tau$. The total addenda consists of the sapphire substrate, the doped silicon heater and thermometers, the aluminum contact pads, the Wakefield thermal compound used to attach the sample to the sapphire, any extra gold wire on the chip, and one-third of the gold wire between the SOS chip and the block.[27] The heat capacity of the addenda is determined separately for each run, and is typically about 0.2 μJ/K at 4.2 K.

Under standard operating conditions, the precision of the measurement in the temperature range 2–10 K is $\sim 0.5\%$. When the addenda heat capacity is determined from the addenda weights and from the previous addenda calibration, the absolute accuracy is limited to $\sim 10\%$. The addenda specific heat is mostly due to phonons, so that the systematic uncertainty corresponds to a $\sim 3\%$ uncertainty in the Debye temperature of the sample. For many runs, a greater absolute accuracy is obtained by measuring the specific heat of the addenda in a separate run before placing the sample on the SOS chip. Measurements of an empty SOS chip suggest that field dependent systematic errors are comparable to the precision of the data, about 1% of the addenda heat capacity over most of the temperature range above 3 K (Fig. 1).

The sample is weighed to the nearest microgram both before and after the measurement to make sure that no chip-

ping or cracking has occured during thermal cycling. The specific heat, c, is reported in units of mJ/mol K, normalized in moles of formula units ($13-\delta$ atoms).

III. CRYSTALS

The single-crystal $YBa_2Cu_3O_{7-\delta}$ samples were grown at the University of British Columbia (UBC) by a flux-growth technique in $BaZrO_3$-coated yttria stabilized zirconia crucibles.[30] Crystals grown by this technique have previously been characterized by low-field magnetization, *ab*-plane resistivity, heat capacity near T_c, and microwave surface resistance. Similar samples show a linear temperature dependence of the microwave penetration depth.[7] The samples chosen for specific heat, while small by the usual standards of heat capacity measurements, were an order of magnitude larger than those used for microwave measurements. The linear-T behavior of the penetration depth was confirmed on smaller samples from the same batch.

The crystals were annealed on YBCO ceramic in a tube furnace under high purity oxygen flow. The pressure and temperature required to achieve particular doping levels had been previously calibrated and checked by titration on ceramic samples. The estimated error in the oxygen doping, δ, is ± 0.005.

Sample T1 was a nominally pure, twinned 2.6 mg single crystal, initially measured at optimal doping, $(7-\delta)=6.95$. The crystal had a transition temperature $T_c=93.1$ K with a width $\Delta T_c<0.2$ K as determined by SQUID magnetometry. Optical and scanning electron microscopy showed the surface and edges of the crystal to be mostly clean, with a few flux spots which occupied $<0.1\%$ of the sample volume. Microprobe analysis showed that the flux spots were $BaCuO_y$. Although the volume of these spots was small, $BaCuO_y$ is known to have a high specific heat,[31] so the zero-field specific heat was remeasured after the flux spots were scraped off the sample. Any change in the sample's specific heat due to the presence of the $BaCuO_y$ was smaller than experimental error. The sample was then cut into pieces: no evidence of impurity inclusions was found.

One of the pieces of sample T1, weighing 0.8 mg, was detwinned to create sample U1. About 20% of the surface of sample U1, near two of the corners, had a high density of visible twins remaining after the detwinning process. Specific heat data were taken on a second nominally pure, twinned single crystal (sample T2). Sample T2 was detwinned to create sample U2, which had fewer visible twin boundaries remaining than sample U1. Both U1 and U2 were reoxygenated to $(7-\delta)=6.95$ subsequent to detwinning. Sample U1 was eventually remeasured after reoxygenation, first to $(7-\delta)=6.97$, and then to $(7-\delta)=6.99$.

IV. DATA

The zero-field specific heats of the UBC crystals T1 (twinned, $7-\delta=6.95$) and U1 (untwinned, $7-\delta=6.95$, 6.97, and 6.99) are plotted in Fig. 2(a) as c/T vs T^2. The increase in the noise in the measurement of U1 relative to T1 results from the sample's smaller size. Two general trends are noticeable from Fig. 2. First, the total specific heat decreases as twin boundaries are removed, and decreases further as oxygen is added. Second, the data are close to linear on a plot of c/T vs T^2, suggesting that the specific heat can be reasonably well described by $c(T,0)=\gamma T+\beta T^3$. Figure 2(b) shows the specific heat of samples T2 (twinned, $7-\delta=6.95$) and U2 (untwinned, $7-\delta=6.95$). These data also appear linear on a plot c/T vs T^2, and the specific heat again decreases as twin boundaries are removed from the sample.

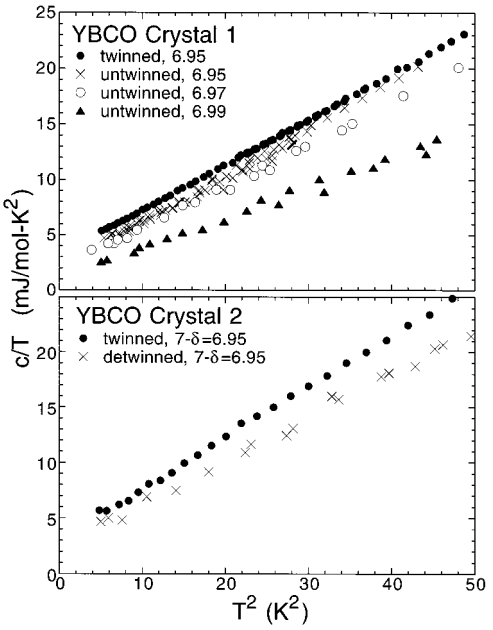

FIG. 2. The zero-field specific heat of two $YBa_2Cu_3O_{7-\delta}$ single crystals, plotted as $c(T,0)/T$ vs T^2, before and after detwinning and reoxygenation.

Figure 3 shows the specific heat of crystal T1 in zero field and in an 8 T magnetic field applied either parallel or perpendicular to the copper oxide planes. The specific heat increases in a magnetic field, and the anisotropy of the field-dependent increase is comparable in magnitude to the total increase. In a separate run, data were taken in an 8 T magnetic field applied in the plane at 0 and 45 degrees to the twin boundaries [Fig. 3 (inset)] on sample T1. No in-plane anisotropic magnetic field dependence was found within the resolution of the measurement. In a magnetic field, the data are not linear on a plot of c/T vs T^2, but show a broad ''bump'' at the lower temperatures. This bump is similar in parallel and perpendicular magnetic fields. In addition, the perpendicular-field data exhibit a close-to-constant offset from the parallel-field data, suggesting an increased linear-T term in perpendicular field.

V. MODELS FOR DATA ANALYSIS

The Debye phonon specific heat, c_D, is cubic in temperature at low temperatures,

$$c_D=\frac{12\pi^4}{5}nk_B\left(\frac{T}{\Theta_D}\right)^3\equiv\beta T^3, \tag{1}$$

where Θ_D is the Debye temperature.[32] At higher temperatures the Debye interpolation is insufficient to describe the phonon specific heat of most materials. The deviations may

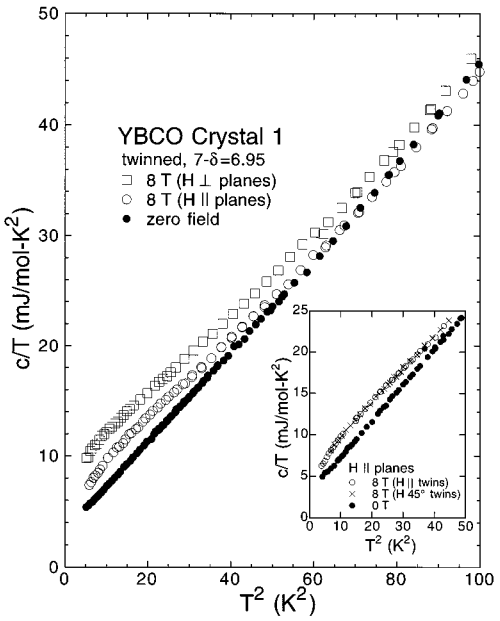

FIG. 3. The specific heat of sample T1, plotted as $c(T,H)/T$ vs T^2, for magnetic fields of 0 T and 8 T applied either parallel or perpendicular to the CuO_2 planes. Inset: Data from a separate run, showing two different orientations of the magnetic field within the plane.

be expanded in higher order terms such as T^5, T^7, etc., assuming that dispersion is the dominant effect. They may also be described as a gapped Einstein contribution, c_E, associated with optical phonons:

$$c_E = mR\left(\frac{T_E}{T}\right)^2 \frac{\exp(-T_E/T)}{[1-\exp(-T_E/T)]^2}, \tag{2}$$

where m is the number of oscillators per unit cell and $R=8314$ mJ/mol K is the universal gas constant. In general, both are expected and a comparison of these approaches is beyond the scope of this paper. We will mostly restrict our discussion to the temperature range $T<8$ K, in which we find empirically that a T^3 term is sufficient to describe the data.

In principle, the phonon specific heat may be field dependent, and both the sound velocity and the density of YBCO have been shown to be field dependent. Measurements of the ''giant magnetostriction'' effect in YBCO show length changes $\Delta L/L$ of order 10^{-4} at 4.2 K in fields up to 12 T,[33] and the sound velocity v_s shows changes of the same order,[34] $\Delta v_s/v_s \sim 10^{-4}$. In an oversimplified model for the phonons, these quantitities can be directly related to the Debye temperature Θ_D, which is proportional to the sound velocity and to the density of the lattice. Thus, these measurements suggest that any field dependence of the phonon specific heat, βT^3, would be more than an order of magnitude below than the resolution of our data.

The low-temperature electronic specific heat of a normal metal obeys

$$c_e = \gamma_n T, \tag{3}$$

where γ_n is proportional to the density of states at the Fermi level, $N(E_F)$.[32] The linearity of the electronic contribution depends on the assumption that the density of states is constant over the energy range probed by the measurement, k_BT. Any energy dependence of the density of states in this range will change the electronic specific heat.

In a superconductor with lines of nodes in the gap function, the density of states $N(E)$ rises linearly with energy at the Fermi level in zero field, $N(E) \propto |E-E_F|$. This density of states results in a contribution to the electronic specific heat c_e which is quadratic in temperature,

$$c_e = \alpha T^2. \tag{4}$$

The coefficient α may be estimated from the slope of the density of states as $\alpha \approx \gamma_n T^2/T_c$, where γ_n is the coefficient of the linear-T term in the normal state,[22–24] neglecting factors assumed to be of order 1 such as angular dependence of the density of states.

The specific heat of most high-T_c materials in a magnetic field contains a broad low-temperature peak which can be well described by a spin-1/2 Schottky anomaly, $nc_{\text{Schottky}}(T,H)$.[19,20] The Schottky anomaly is given by

$$c_{\text{Schottky}}(T,H) = \left(\frac{g\mu_B H}{k_B T}\right)^2 \frac{e^{g\mu_B H/k_B T}}{(1+e^{g\mu_B H/k_B T})^2}, \tag{5}$$

where μ_B is the Bohr magneton and g is the Landé g factor. The concentration of spin-1/2 particles is n/R, where R is the universal gas constant. This expression is exact only for free spins. The number of spins needed to describe the specific heat of cuprate superconductors has variously been argued to be linear in field in YBCO;[35] to be linear in field at low fields and relatively constant at high fields in LSCO;[36] and to be field independent in YBCO.[37] The apparent field dependence of the number of spins depends, of course, on which other terms are allowed in the description of the total field-dependent specific heat.

The Landé g factor may be somewhat anisotropic, and spin-spin interactions may broaden the Schottky anomaly. In zero field, there is no contribution to the specific heat from ideal free spin-1/2 particles. The presence of internal fields or interactions between the spin-1/2 particles may result in a broadened Schottky anomaly. This broadening is more noticeable at low fields and low temperatures, where it appears as an upturn in the zero-field low-temperature specific heat. Some techniques for describing the broadening have been discussed by the Berkeley group.[20,37,38] Depending on the temperature range, several parameters may be required to model the upturn, or it may be possible to represent it as the high-temperature tail of a Schottky anomaly with some effective internal field H_{eff},

$$c_{\text{Schottky}}(T,H\approx 0) = \frac{1}{4}\left(\frac{g\mu H_{\text{eff}}}{k_B T}\right)^2. \tag{6}$$

Cuprate superconductors are strongly type-II materials, and there are several possible contributions associated with vortices in the mixed state. In 1964 Caroli, deGennes, and Matricon[39] showed that the quasiparticle excitations inside the vortex core have an energy level spacing $\varepsilon_0 \approx \Delta^2/E_F$. The core ''minigap'' ε_0 is comparable to the energy level spacing of an electron confined to a box of size ξ. At very

low temperatures, this energy level spacing theoretically results in a gapped contribution to the specific heat,[40]

$$c_{\text{cores}} \approx \gamma_n T \frac{H}{H_{c2}} \left(\frac{\varepsilon_0}{k_B T} \right)^{5/2} e^{-\varepsilon_0 / k_B T}, \quad k_B T \ll \varepsilon_0 . \tag{7}$$

The minigap is quite low for conventional superconductors, but can be calculated to be tens of K or more for cuprate superconductors due to their short coherence length. At temperatures large compared to the minigap, $k_B T \gg \varepsilon_0$, the vortex core behaves much like a cylinder of normal metal with radius ξ. In this case the temperature dependence of the specific heat is similar to that of a normal metal,[40]

$$c_{\text{cores}} = \gamma(H) T \approx \gamma_n T \frac{H}{H_{c2}}, \quad k_B T \gg \varepsilon_0 . \tag{8}$$

Equations (7) and (8) have quite different temperature dependences, but share a common field dependence. H/H_{c2} may be roughly interpreted as the volume fraction of the ''normal'' cores. In general, for isolated vortex cores, any contribution from excitations inside the cores will increase linearly with the number of cores. Thus, any core contribution will be linear in H for $H_{c1} \ll H \ll H_{c2}$. This discussion about the core contribution is based on the assumption $\lambda \gg \xi$, and therefore only hold for high-κ materials. In materials which are not strongly type II, the vortex cores cannot be treated as isolated. Neither Eq. (7) nor Eq. (8) provides a good description of the measured $\gamma(H)$ of, for example, vanadium.[41]

In addition to contributions associated with the internal degrees of freedom, it is possible to excite modes associated with vortex-vortex interactions.[42–44] In a layered superconductor, neglecting damping, the vortex mass, and interlayer coupling, these modes would result in a two-dimensional Debye specific heat with a vortex Debye temperature $\Theta_v = \frac{1}{2} \hbar \omega_c / k_B \approx 7$ K for $B = 10$ T.[44] In this model, the low-temperature specific heat varies as T^2, as expected for a two-dimensional Debye solid, and saturates at temperatures above Θ_v to the classical limit of 1 k_B per pancake. The detailed functional dependence in the presence of finite dissipation, mass, and Magnus force has been discussed in several theoretical papers.[42–44] An unambiguous identification of the vortex lattice specific heat would provide an important test of phenomenological models of vortex dynamics. All of these models share the common feature that the specific heat saturates to the classical Dulong and Petit limit of 2 k_B per pancake at most, which is within current experimental resolution. When the isolated pancake description is not valid, and interlayer coupling is introduced, such as would be appropriate for YBCO, the number of degrees of freedom may be reduced by orders of magnitude from this limit.

In two high-κ A15 compounds, the coefficient of the linear-T term in the specific heat has been shown by Stewart and Brandt to be linear in H.[45] The coefficient of the linear-T term for V_3Si was slightly larger than expected from Eq. (8), but Eq. (8) provides a good description of the magnetic field dependence of the specific heat for Nb_3Sn. More recently, in zero-field-cooled measurements of V_3Si, Ramirez has found hysteresis and curvature in the field dependence of the specific heat near H_{c1}, suggesting that the field dependence of the specific heat of conventional high-κ materials is not fully understood near H_{c1}.[46]

The estimated minigap for the cuprate superconductors is sufficiently large that the condition $k_B T \gg \varepsilon_0$ is not satisfied in the Caroli-deGennes-Matricon model. There is some experimental evidence for a large minigap,[47,48] although a consensus has not been reached. Although Eq. (8) is thus not expected to apply to the cuprates, Fig. 3 shows that the increase in the specific heat in a magnetic field is not exponentially suppressed at low temperatures and is much larger than can be explained by a minigap core contribution, Eq. 7. If there is a minigap core contribution to this specific heat data, it is too small to identify in the presence of the other excitations.

Caroli, deGennes, and Matricon assumed a fully gapped superconductor in their calculations.[39] Volovik calculated in 1993 that for a superconductor with lines of nodes in the gap function, the dominant contribution to the magnetic field dependence of the specific heat should come from quasiparticle excitations *outside* the vortex core.[26] The density of states predicted by Volovik results from the Doppler shift of the quasiparticle excitation spectrum in the presence of a nonzero supercurrent. If the superfluid velocity is $\vec{v_s}$, the quasiparticle excitation spectrum $E(\vec{k}) = \sqrt{\eta_k^2 + |\Delta_k|^2}$, where η_k is the bare excitation energy and Δ_k is the superconducting energy gap, is shifted by an amount $\vec{k} \cdot \vec{v_s}$. This shift is the physical origin of the depairing current. Far from the vortex core in a fully gapped superconductor, the Doppler shift $\vec{k} \cdot \vec{v_s}$ is small compared to the gap, and does not have much effect on the excitation spectrum. Within a coherence length of the core, however, the Doppler shift is comparable to the gap, and significant pairbreaking results. This effect is one way to understand the conventional normal-core model.

Volovik's result[26] is derived from the Doppler shift and from the dependence of the intervortex spacing $R(H)$ on magnetic field, $R(H) \propto 1/\sqrt{H}$. The density of states at the Fermi level is related to the quasiparticle excitation energy $E(\vec{k})$ by

$$N(E_F) = \int \frac{d^3k}{(2\pi)^3} \int d^2r \, \delta(E(\vec{k},\vec{r}) - \vec{k} \cdot \vec{v_s}(\vec{r})). \tag{9}$$

For a superconductor with lines of nodes, the shift is significant everywhere that the superfluid velocity is not zero. The vortex superfluid velocity v_s depends on the distance r from the center of the vortex as $v_s \propto 1/r$. The integrand in Eq. (9) may be loosely interpreted as the local density of states at the Fermi level, which thus falls off as $1/r$ and has an angular variation which reflects the symmetry of the underlying order parameter. This local density of states is plotted in Fig. 9 for a tetragonal d-wave gap function.

To find the total density of states, Eq. (9) is integrated over the entire vortex. For $H \gg H_{c1}$, i.e., $R(H) \ll \lambda$, the intervortex spacing $R(H)$ is the upper cutoff in the integral. This integral gives a density of states per vortex $N(E_F,H) \propto R(H) \propto 1/\sqrt{H}$. In the limit that the number of vortices is proportional to H, which is not valid near H_{c1}, multiplying by the number of vortices gives a total density of states $N(E_F,H) \propto \sqrt{H}$. Finally, noting that the density of states should extrapolate roughly to the normal-state density of states N_n at $H = H_{c2}$, this result is normalized as

$$N(E_F,H)=kN_n\sqrt{H/H_{c2}}, \tag{10}$$

where k is a factor of order 1. The factor k has not been quantitatively calculated, but should depend on the vortex lattice structure, on the slope of the gap near the gap node, and on possible structure in N_n.

The shift in the excitation spectrum depends on the angle between the local superfluid velocity and the nodes, giving the vortex the same symmetry as the gap (Fig. 9). Because the nodes are 90° apart (in a purely tetragonal d-wave superconductor), the superfluid velocity can never be perpendicular to all nodes, and there are no places where $N(E_F)$ becomes zero. Both the density of states, and in a clean system the anisotropy in the density of states, extend throughout the entire vortex.

As the field is increased, the node fills in with a finite density of states, and the αT^2 term associated with the nodes is replaced by a linear-T term,

$$c_{\text{Volovik}}=k\gamma_n T\sqrt{H/H_{c2}}. \tag{11}$$

Depending on the field and temperature, it may be possible to observe a crossover between these two behaviors.

There is presently a great deal of interesting theoretical activity concerning the influence of anisotropic gaps on the structure of the vortex core.[49–51] The theoretically complicated core structure would modify the $\sqrt{H}$ term except in the limit $H\ll H_{c2}$. The Volovik term comes predominantly from the region between the cores, so the observation of the Volovik term at intermediate fields would not give direct information about the core structure.

VI. ANALYSIS OF ZERO-FIELD DATA

Since the absolute scatter (in units of mJ/mol K) increases at higher temperatures, a weighted-least-squares criterion was used for all fits,

$$\text{minimize}\sum\left(\frac{c_{\text{fit}}-c_i}{c_i}\right)^2. \tag{12}$$

The quoted errors are only statistical and are determined at the 90% confidence level by bootstrapping.[52]

The dependence of the specific heat on twinning and oxygen doping may be seen in Fig. 2, where the specific heat of crystals T1, U1, T2, and U2 are plotted as c/T vs T^2. These data may be fit to straight lines, $c(T,0)/T=\gamma(0)+\beta(0)T^2$, giving the values found in Table I and plotted in Fig. 4. The largest measured value of $\gamma(0)$ from the data in Table I is 3.2 mJ/mol K^2, and this term decreases as twins are removed and further decreases as oxygen is added. Most YBCO samples have zero-field linear-T terms with coefficients $\gamma(0)\geqslant 4$ mJ/mol K^2.[20,19]

Although the specific heat data for sample T1 shown in Fig. 2 is well described by $c(T,0)=\gamma(0)T+\beta T^3$, one cannot rule out the possibility that the specific heat may include other terms. Physically motivated possibilities include a quadratic term αT^2 associated with lines of nodes and a small low-temperature upturn A_2/T^2. A large upturn associated with spin-spin interactions for spin-1/2 particles, Eq. (6), is usually seen in the low-temperature specific heat of $YBa_2Cu_3O_{7-\delta}$.[37] For data plotted as c/T vs T^2, an A_2/T^2 would result in an upturn at low temperatures, while an αT^2 term would result in a downturn. It is possible for both terms to be present with small coefficients, without being obvious in a visual inspection of a graph such as Fig. 2.

TABLE I. Zero-field specific heat fit to $c/T=\gamma+\beta T^3$. Units are mJ, mol, and K.

Sample	$7-\delta$	$\beta(0)$	$\gamma(0)$
T1[a]	6.95	0.405 ± 0.001	3.23 ± 0.03
U1[b]	6.95	0.400 ± 0.010	2.2 ± 0.1
U1[b]	6.97	0.367 ± 0.010	2.0 ± 0.2
U1[b]	6.99	0.265 ± 0.010	1.2 ± 0.1
T2[a]	6.95	0.460 ± 0.010	3.0 ± 0.2
U2[b]	6.95	0.387 +0.020−0.014	2.4 +0.4−0.5

[a]Twinned.
[b]Mostly untwinned.

To set limits on these terms, the data is fit to the functional form,

$$c(T,0)=A_2/T^2+\gamma(0)T+\alpha T^2+\beta T^3. \tag{13}$$

The results of the fit to Eq. (13), and variations on this equation with α and/or A_2 chosen to be zero, are shown in Table II. Four parameters is quite a few for the description of a single smooth data set, and either zero or small values of both α and A_2 are consistent with the data.

The value $\beta=0.40$ mJ/mol K^4 corresponds to a Debye temperature $\Theta_D=400$ K. The values of β in Table I are comparable to what have been observed in other measurements.[20,19] The change in β with oxygen content corresponds to a 10% change in Θ_D. A similar dependence of β on oxygen content has also been observed by Nakazawa and Ishikawa.[53] Fits from 2 to 4 K and from 4 to 7 K give the same value of β within statistical error, indicating that higher

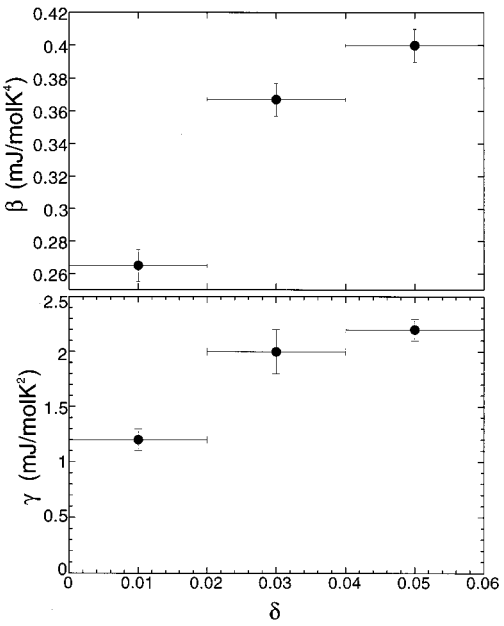

FIG. 4. Dependence of the specific heat parameters on oxygen content for the mostly untwinned crystal U1.

TABLE II. Fits to Eq. (13) for sample T1 from 2–7 K. Units are mJ, mol, K, and T.

rms (%)	$\gamma(0)$	β	α	A_2
0.44	$2.7+0.5-0.3$	$0.394+0.015-0.014$	$0.16+0.13-0.16$	$3.5+1.4-2.6$
0.45	$3.11+0.06-0.04$	0.409 ± 0.002		$1.9+0.6-1.2$
0.48	$3.48+0.16-0.18$	0.421 ± 0.009	-0.13 ± -0.08	
0.52	3.23 ± 0.03	$0.405+0.002-0.001$		

powers of temperature are not necessary to describe the data. Above 8 K, the specific heat deviates from a T^3 law. These deviations are consistent with either higher order terms in the phonon specific heat such as T^5 and T^7, or with a gapped excitation. Several forms of gapped excitations, including a spin gap and an optical phonon mode [Eq. (2)], give adequate descriptions of the data. When the optical phonon form is used, the fit results in the value $T_{\rm gap}\approx 90$ K. In order to avoid the extra parameters necessary to describe the phonon specific heat above 8 K, all of the remaining fits reported here are restricted to $T\leqslant 7$ K.

VII. ANALYSIS OF THE FIELD DEPENDENCE

Figure 3 shows the specific heat of crystal T1 in zero field and in an 8 T magnetic field applied either parallel or perpendicular to the copper oxide planes. The largest contribution to the specific heat is the βT^3 term, believed to come from the Debye phonons. All three data sets have similar slopes on this plot of c/T vs T^2, indicating that the βT^3 term is similar in all three data sets. The zero-field linear-T term $\gamma(0)T$ appears as a finite intercept on the c/T axis for the zero-field data. In an 8 T magnetic field applied parallel to the CuO_2 planes, there is an additional magnetic contribution, a low-temperature bump peaking around 3–4 K. In an 8 T perpendicular magnetic field, there is a similar bump. As discussed below and previously shown by Emerson *et al.* for polycrystalline samples,[37] this contribution can be well described as a Schottky anomaly, $nc_{\rm Schottky}(T,H)$, due to an assumed concentration of spin-1/2 particles. The data in perpendicular field also show a substantially increased linear-T term, $\gamma_\perp(H)T$.

The approximately linear-T temperature dependence of the anisotropy of the specific heat cannot be explained by a contribution from vibrations of the vortex lattice, which should level out at a temperature-independent value of 1 or 2 k_B per pancake at a temperature of a few K in an 8 T field. In fact this upper limit is generous, since it assumes that the vortex has a mass for the $2k_B$ limit and that the pancake vortices are decoupled. Even with these assumptions, the upper limit $2k_B$ per pancake is too small to explain the observed anisotropy of the field dependence of the specific heat.

The anisotropic magnetic field dependence is also much larger than can be explained by a minigap core contribution, Eq. (7), with a minigap of tens of K or more as expected for YBCO. In order to explain the approximately linear-T dependence of the anisotropy, the minigap would need to be small compared to the temperature range of the measurements, and Eq. (8) would then apply for a traditional high-κ superconductor. While a gapped core may be present, the specific heat of such cores is insufficient to explain the data.

Accordingly, we model the data allowing for the other contributions mentioned in the last section: a possibly anisotropic Schottky anomaly, and a linear-T term with an unknown H dependence. Each data set at each value of the magnetic field is thus described by

$$c(T,H)=\gamma T+\beta T^3+nc_{\rm Schottky}(g\mu_B H/k_B T). \qquad (14)$$

The specific heat data in zero magnetic field and in two orientations of an 8 T applied field (Fig. 3) are replotted in Fig. 5(b) with the phonon specific heat subtracted. This plot shows that the location of the maximum of the Schottky anomaly is slightly different in the two curves. The data in parallel and perpendicular fields can be fit to Eq. (14) with the Landé g factor treated as a free parameter. This fit results in the values $g_\perp=2.0$ for a field applied perpendicular to the CuO_2 planes and $g_\parallel=2.2-2.3$ for a field applied parallel to the CuO_2 planes. The data on sample T1 in an 8 T parallel field show a linear-T term, $\gamma_\parallel(H)T$, which is increased by about 0.5 mJ/mol K^2 relative to $\gamma(0)$, as determined by fitting the data in Figs. 5(a) to Eq. (14). Because of uncertainties in the Schottky anomaly and the sample alignment, the results are also consistent with no increase in the parallel-field linear term, $\gamma_\parallel(H)T$.

We now turn our attention to the perpendicular field. Each of six data sets (H = 0, 0.5, 2, 4, 6, and 8 T) from sample T1 is fit individually to Eq. (14), using a Landé g factor of $g=2$. As in the last section, a weighted-least-squares criterion was used for all fits. The parameters resulting from this fit are listed in Table III and are plotted in Fig. 6, along with statistical error bars determined at the 90% confidence level by bootstrapping. The importance of bootstrapping is shown by the error bars in Fig. 6. Although all data sets are of similar quality, the dependence of the parameters on each other and on different temperature ranges depends on the field. Accordingly, the error bars vary considerably with field.

TABLE III. Individual-field fits to Eq. (14) for sample T1 from 2–7 K. Units are mJ, mol, K, and T.

H	γ	β	n
0.0	$3.23+0.03-0.03$	$0.405+0.002-0.001$	
0.5	$3.58+0.09-0.09$	$0.397+0.002-0.003$	$43+20-23$
2.0	$4.32+0.10-0.09$	$0.388+0.003-0.004$	$26.1+1.0-0.9$
4.0	$5.23+0.20-0.19$	$0.389+0.006-0.005$	$21.9+1.0-1.3$
6.0	$4.77+0.63-0.88$	$0.402+0.019-0.012$	$25.9+5.1-4.2$
8.0	$6.16+0.51-0.41$	$0.386+0.005-0.007$	$19.0+3.2-3.9$

Of the three parameters, γ, β, and n, only γ has a strong magnetic field dependence, increasing with H with negative

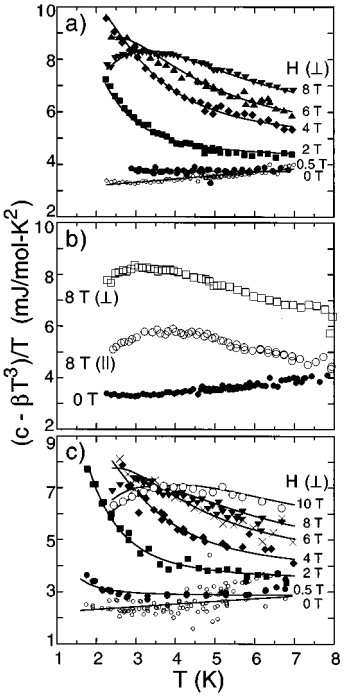

FIG. 5. ''Nonphonon'' specific heat in various magnetic fields, plotted as $(c-\beta T^3)/T$ vs T. The solid lines are the global fit described in Sec. V. (a) Crystal T1, $H\perp$ planes, $\beta=0.392$. (b) Crystal T1, $H\perp$ or $\|$ planes, $\beta=0.392$. (c) Crystal U1, $H\perp$ planes, $\beta=0.380$.

curvature. The larger apparent value of n for $H=0.5$ T may be physically explained by interactions between the spin-1/2 particles, but is not statistically significant. Within the resolution of the measurement, β is independent of field for

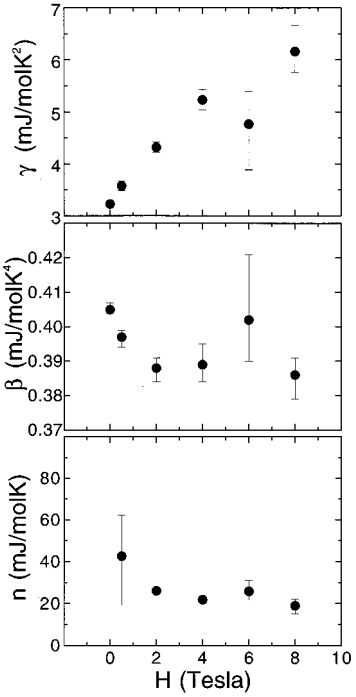

FIG. 6. Parameters from fitting six different data sets on crystal T1 in perpendicular field to $c=\gamma T+\beta T^3+nc_{\text{Schottky}}$. Error bars are at the statistical 90 % confidence level.

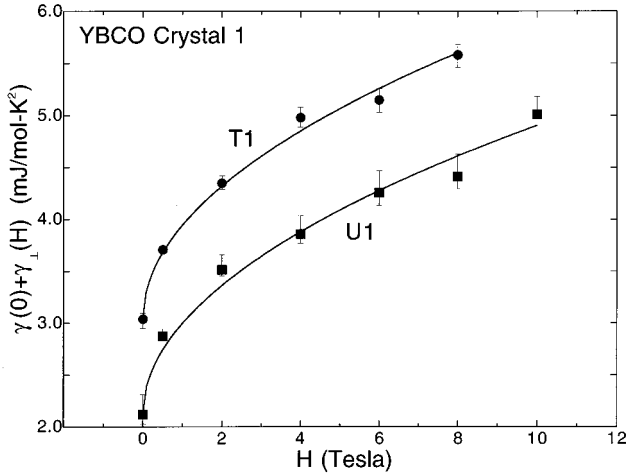

FIG. 7. Field dependence of the coefficient of the linear-T term for crystals T1 (twinned) and U1 (mostly untwinned), as determined from a global fit. Error bars are at the statistical 90% confidence level. The solid lines are fits to $\gamma(0)+A\sqrt{H}$. T1: $\gamma(0)=3.04$ mJ/mol K^2 and $A=0.91$ mJ/mol K^2 T$^{1/2}$. U1: $\gamma(0)=2.12$ mJ/mol K^2 and $A=0.88$ mJ/mol K^2 T$^{1/2}$.

$H\geqslant 2$ T, and is increased by $\sim 5\%$ in zero field. No quadratic term was allowed in this fit. As is discussed in detail later, a quadratic term associated with lines of nodes would be about 5% of the phonon specific heat in this temperature range, would be difficult to separate from a βT^3 term in zero field, and would be expected to disappear in a magnetic field.

The scatter in the values of β, n, and γ is partially due to the large number of parameters (three) used to describe each data set. These results suggest that it is appropriate to refit the data with the assumptions of the field independence of

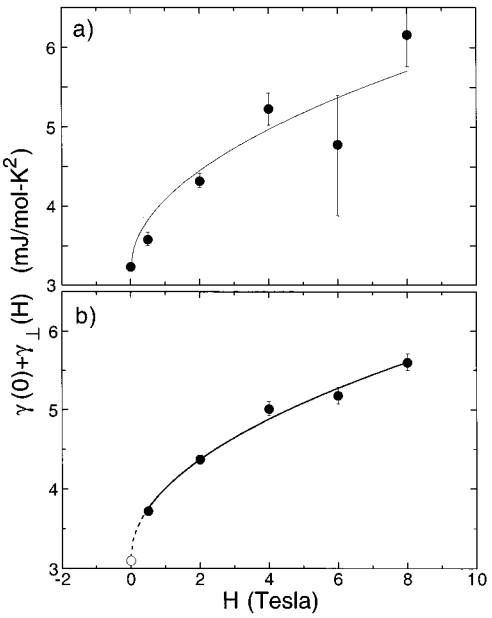

FIG. 8. Coefficient of the linear-T term for crystal T1, as determined from (a) individual-field fits and (b) a global fit with the $H=0$ data set excluded. The solid lines are fits to $\gamma(0)+A\sqrt{H}$ with $A=0.89$ mJ/mol K^2 T$^{1/2}$ and $A=0.87$ mJ/mol K^2 T$^{1/2}$, respectively.

TABLE IV. Global fit parameters for samples T1 and U1. Units are mJ, mol, K, and T.

	Sample T1	Sample U1
$\gamma(0)$	3.0 ± 0.1	$2.1+0.1-0.2$
n	24 ± 1	23 ± 1
β	0.392 ± 0.001	0.380 ± 0.004
α	0.11 ± 0.02	0.10 ± 0.06
$\gamma_\perp(H)$	$0.91\sqrt{H}$	$0.88\sqrt{H}$

the concentration of spin-$\frac{1}{2}$ particles, n, and the phonon specific heat, βT^3. In addition to being consistent with the individual-field fits, these assumptions are physically plausible, as discussed in Sec. IV. To model the perpendicular field dependence with such constraints, identical analyses are performed on data from samples T1 (twinned) and U1 (untwinned). Allowing for the possibility of a small quadratic term, αT^2, the zero-field specific heat is described by

$$c(T,0)=\gamma(0)T+\alpha T^2+\beta T^3. \tag{15}$$

The specific heat for $H\geqslant0.5$ T is described by

$$c(T,H)=[\gamma(0)+\gamma_\perp(H)]T+\beta T^3+nc_{\text{Schottky}}(g\mu_B H/k_B T). \tag{16}$$

All data sets are fit simultaneously to Eqs. (15) and (16) with a Landé g factor of $g=2.0$. In this global fit, β and n are constrained by multiple data sets, $\gamma(0)$ and α are constrained by the zero-field data, and $\gamma_\perp(H)T$ is allowed a different value at each field.

The parameters determined from this fit are shown in Table IV for both samples T1 and U1, with 90% statistical confidence levels. The coefficient of the Schottky anomaly, n, indicates 0.1% spin-1/2 particles per copper. The difference in the Debye term between the two samples is within the systematic error of the Debye term of the addenda. The rms deviation of the data from the fit is 0.8% for T1 and 2.7% for U1. The higher scatter in the data for the untwinned crystal U1 results from the smaller sample size. The data and fits for samples T1 and U1 are shown in Fig. 5, with the phonon specific heat (βT^3) subtracted.

The field-dependent linear-T term, $\gamma_\perp(H)T$, has a nonlinear dependence on field (Fig. 7). This nonlinear field dependence is well described by $\gamma_\perp(H)=A\sqrt{H}$, with $A=0.9$ mJ/mol K^2 T$^{1/2}$ for both samples T1 and U1.

The qualitative nonlinearity of $\gamma_\perp(H)$ is robust to the assumptions used to describe the total specific heat. The coefficients of the linear-T term for sample T1 as determined from the individual fits (Fig. 6) are replotted in Fig. 8(a), together with a fit to $\gamma(0)+\gamma_\perp(H)=\gamma(0)+A\sqrt{H}$. This fit results in the value $A=0.89$ mJ/mol K^2 T$^{1/2}$, as was also found in the global fit.

In an alternative fit which avoids the zero-field data entirely, the five data sets for sample T1 with $H\geqslant0.5$ T are globally fit to Eq. (16), again keeping β and n independent of field. There are thus two global parameters, plus values of $[\gamma(0)+\gamma_\perp(H)]$ in five fields [Fig. 8(b)]. The resulting linear-T term is better described by a $\sqrt{H}$ dependence than by an H dependence, and from the fit shown in Fig. 8(b), $A=0.87$ mJ/mol K^2 T$^{1/2}$. This fit also returns an extrapolated value of $\gamma(0)=3.1$ mJ/mol K^2, which is in agreement with the value determined by independently fitting just the zero-field data.

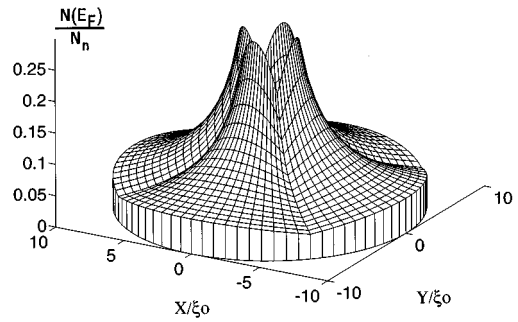

FIG. 9. Schematic of the local density of states $N(E_F)/N_n$ throughout a d-wave vortex, with the core region omitted.

VIII. INTERPRETATION

Any excitations which are confined to the vortex cores would probably result in a contribution to the specific heat which is linear in H (proportional to the number of vortices), independently of the details of the core excitation spectrum. Although there may in principle be some dependence of the core excitations on magnetic field, it is likely that for $H\ll H_{c2}$ the core excitations would be roughly independent of field. Accordingly, a nonlinear field dependence observed in $N(E_F,H)$, such as we observe, suggests excitations outside the vortex core. The observed field dependence of the specific heat agrees semiquantitatively with the prediction of Volovik for the density of states at the Fermi level for a superconductor with lines of nodes in the gap function.[26] This density of states extends throughout the entire vortex (Fig. 9).

Parks *et al.* have pointed out that their measurements of vortex dynamics in YBCO thin films are best explained by the presence of the extra quasiparticles expected for a vortex with an anisotropic gap.[54] Recent theoretical work suggests that the structure of the vortex core in a d-wave superconductor is both interesting and complicated,[26,49–51] containing a gradient-induced s-wave component of the order parameter. We are not aware of any model for the core which suggests that the core region contains enough excitations to explain our results, or which suggests a core contribution to the specific heat with a nonlinear dependence on field for $H\ll H_{c2}$. The core region has been deliberately omitted from Fig. 9, since at the present time it appears that the specific heat is not a measure of the core states.

Theoretically, $N(E_F,H)$ depends on the orientation of the current with respect to the nodes. High-resolution measurements of the full angular dependence $\gamma_{\theta,\varphi}(H)T$ should be sensitive to the positions of the nodes. The full angular dependence has been calculated quantitatively by Volovik in an anisotropic Ginsburg-Landau theory for a tetragonal $d_{x^2-y^2}$ gap function.[55] For a magnetic field $\vec{H}$ parallel to a node, the currents in the a–b plane are also flowing parallel to two nodes, but are orthogonal to the other two. The density of states at the Fermi level is $\sqrt{2}$ larger when the currents flow parallel to the antinodes: in this orientation, the density of

states picks up contributions from all of the nodes. The complete in-plane angular magnetic field dependence of the density of states is given by

$$N(0,H,\theta=\pi/2,\varphi)=\frac{\kappa'}{2}(|\sin\varphi|+|\cos\varphi|)N_F\sqrt{H/H_{c2\|}}, \tag{17}$$

as shown by Volovik.[55]

Measurements of the in-plane anisotropy of the magnetic field dependence at 8 T were made on a heavily twinned sample of $YBa_2Cu_3O_{6.95}$ with the field parallel to the twins and at a 45° angle to the twins [Fig. 3 (inset)]. These measurements did not detect a significant angular variation in $\gamma_\|(H)$ within the experimental error (about 0.2 mJ/mol K^2).

To compare these results to theory requires a value for $H_{c2||}$, which is not well known. Guessing $H_{c2||}=1000$ T, consistent with measurements of $H_{c2\perp}$ and the anisotropy, and taking $\gamma_n\simeq 20$ mJ/mol K^2 as found in other heat capacity measurements,[20,21] Eq. (17) gives an estimated angular variation of 0.4 mJ/mol K^2 times a factor of order 1 for a purely tetragonal d-wave superconductor. The theoretical uncertainties are sufficiently large that these data are not evidence against an anisotropic gap, although the estimated in-plane anisotropy and the resolution of the measurements are comparable in magnitude. Measurements at higher fields over a greater range of angles, preferably on untwinned samples, might improve our understanding of the structure of in-plane vortices, and would allow the determination of the locations of the gap minima if the above model proves to be the correct one.

A quadratic term, αT^2, associated with lines of nodes would be expected to disappear in a magnetic field, where the energy dependence of the density of states close to the nodes, $N(E,H=0)\propto|E-E_F|$, is replaced by a finite $N(E_F,H)$. The field at which this crossover occurs depends on the temperature range. As a rough estimate, the αT^2 term would disappear for crossover temperatures T^* or fields H^* given by $T^*\approx T_c N(E_F,H^*)/N_n\approx T_c\sqrt{(H^*/H_{c2})}$: a little below 0.5 T for the temperature range of these data. The αT^2 term is comparable in magnitude to the systematic uncertainty in the addenda T^3 phonon specific heat, but is several times larger than the relatively small systematic uncertainty of the field dependence, $<1\%$. The individual-field fits which allowed no αT^2 term resulted in an apparent field dependence of the βT^3 term, with $\beta(H=0)$ being increased by about 5%. The global fit, which allowed an αT^2 term in zero field, found $\alpha=0.1$ mJ/mol K^2, such that the zero-field quadratic term was about 5% of the phonon specific heat. The slight positive slope of the zero-field data set in Fig. 5(b) can be described either as a phonon term which is about 5% larger in zero field, which is difficult to explain, or as an αT^2 term that is electronic in origin.

From the slope of the density of states in a superconductor with lines of nodes, theory yields $\alpha\approx\gamma_n/T_c$,[22,23] or $\alpha\approx 0.2$ mJ/mol K^3 for YBCO within factors of order unity. This estimate is in good agreement with the value $\alpha=0.1$ mJ/mol K^3 obtained from the global fits (Table IV) on samples U1 and T1.

For the field dependence of the density of states, Volovik predicts $N(E_F,H)=kN_n\sqrt{H/H_{c2}}$, where k is of order 1 and is defined by the vortex lattice structure, by the slope of the gap near the gap node, and by possible structure in the normal-state density of states N_n.[26] Taking $\gamma_n=20$ mJ/mol K^2, consistent with other heat capacity work,[20,21] and $H_{c2,\perp}=150$ T gives the estimate $\gamma_\perp(H)=A\sqrt{H}$ with $A=k\times 1.6$ mJ/mol K^2 $T^{1/2}$, in reasonable agreement with the value $A=0.9$ mJ/mol K^2 $T^{1/2}$ found for both samples U1 and T1.

Both of the above comparisons used the measured value of γ_n, the normal state density of states averaged over the Fermi surface. Because both the αT^2 and $A\sqrt{H}T$ terms are a consequence of the nodes, these terms should be sensitive to the normal-state density of states close to the nodes. The above comparisons may indicate that the density of states close to the nodes is smaller than the angular average of the density of states, consistent with photoemission measurements on BSCCO:[56] but the theoretical uncertainty in k makes quantitative comparison difficult.

A quadratic T^2 term has been known for some time in the specific heat of heavy-fermion superconductors, and has recently been reported in the specific heat of $La_{2-x}Sr_xCuO_4$.[57] Two other recent works support the existence of a $\sqrt{H}$ term in superconductors with lines of nodes. A $\sqrt{H}$ term has been recently reported in the low-temperature specific heat of UPt_3.[58] Also, a reanalysis of existing data on polycrystalline YBCO samples shows a nonlinear $\gamma(H)T$ term which appears consistent with $\sqrt{H}$,[38] with similar but less dramatic curvature on Ca- and Sr-doped La_2CuO_4 samples.

These predictions do not distinguish between different types of lines of nodes, such as d-wave or extended s-wave.[59] In principle, this interpretation could also apply to a gap function with no nodes, but with a very small minimum gap, $\Delta_{\min}\ll k_BT\approx 0.5$ meV. In order to produce these results, however, such a gap function would need to have an unusual energy dependence of the density of states similar to that associated with lines of nodes, $N(E,H=0)\propto|E-E_F|$.

The above discussion should not be taken to suggest that the data are entirely consistent with the specific heat expected for a superconductor with lines of nodes in the gap function. In fact, the observed zero-field linear-T term is not. A wide range of values have been reported for γ_n, the coefficient of the linear-T term in the normal state of optimally-doped YBCO.[19–21] The later measurements, including the measurements of Loram *et al.*,[21] are close to $\gamma_n=20$ mJ/mol K^2. γ_n is determined from bulk measurements in the normal state and therefore reflects the normal density of states N_n averaged over the entire Fermi surface. In other words, as usually measured, γ_n is not sensitive to possible $\vec{k}$ dependence of N_n. Taking the value $\gamma_n=20$ mJ/mol K^2 with that caveat, the residual density of states $N(E_F)/N_n$ in the superconducting state is about 15% for the twinned samples and drops to $\sim 7\%$ with detwinning and oxygenation (Table I).

The residual density of states can also be extracted from fitting the temperature dependence of the penetration depth[7] to the d-wave model with scattering of Hirschfeld *et al.*[60] In samples similar to the samples measured here, these fits im-

ply a density of states which is no greater than 1% of N_n.[61] It appears difficult to quantitatively reconcile the zero-field linear term $\gamma(0)T$ with the αT^2 and $A\sqrt{H}T$ terms, and with the interpretation of the temperature dependence of the penetration depth.

IX. SUMMARY

The coefficient of the linear-T term in the specific heat of YBCO does not depend linearly on magnetic field, H. The observed curvature with field can be well described by $\sqrt{H}$, with a numerical prefactor which agrees semiquantitatively with Volovik's prediction for the density of states in superconductors with lines of nodes in the gap function.

It is possible that the zero-field linear-T term has a separate origin from the excitations which give rise to the quadratic-T term and to the $\sqrt{H}T$ field dependence of the specific heat. This assumption leads to a self-consistent analysis of the specific heat, and is given additional support by the measurements on the untwinned crystal U1, in which $\gamma(0)$ decreases substantially, while the field-dependent specific heat is unaffected.

ACKNOWLEDGMENTS

Work at Stanford was supported by the Air Force Office of Scientific Research. We thank N. E. Phillips, R. A. Fisher, J. E. Gordon, and A. Junod for extensive discussions, including discussions of their data and analyses prior to publication. We also thank D. A. Bonn, B. Efron, K. Maki, R. B. Laughlin, D. Scalapino, C. Varma, and especially G. Volovik for useful discussions.

*Present address: Department of Physics, Princeton University, Princeton, NJ 08544.

†Present address: Department of Physics, Georgetown University, Washington, DC 20057.

[1] J. Bardeen, L. N. Cooper, and J. R. Schrieffer, Phys. Rev. **108**, 1175 (1957).

[2] N. E. Phillips, Phys. Rev. **114**, 676 (1959).

[3] W. S. Corak, B. B. Goodman, C. B. Satterthwaite, and A. Wexler, Phys. Rev. **102**, 656 (1956).

[4] N. E. Phillips, CRC Crit. Rev. Solid State Sci. 467 (1971).

[5] D. Scalapino, Phys. Rep. **250**, 329 (1995).

[6] D. Pines and P. Monthoux, J. Phys. Chem. Solids **56**, 1651 (1995).

[7] W. N. Hardy, D. A. Bonn, D.C. Morgan, Ruixing Liang, and Kuan Zhang, Phys. Rev. Lett. **70**, 3999 (1993).

[8] D. A. Bonn, S. Kamal, Kuan Zhang, Ruixing Liang, D. J. Baar, E. Klein, and W. N. Hardy, Phys. Rev. B **50**, 4051 (1994).

[9] J. A. Martindale, S. E. Barrett, K. E. O'Hara, C. P. Slichter, W. C. Lee, and D. M. Ginsberg, Phys. Rev. B **47**, 9155 (1993).

[10] Z.-X. Shen, D. S. Dessau, B. O. Wells, D. M. King, W. E. Spicer, A. J. Arko, D. Marshall, L. W. Lombardo, A. Kapitulnik, P. Dickinson, and S. Doniach, Phys. Rev. Lett. **70**, 1553 (1993).

[11] K. A. Moler, D. J. Baar, J. S. Urbach, Ruixing Liang, W. N. Hardy, and A. Kapitulnik, Phys. Rev. Lett. **73**, 2744 (1994).

[12] T. P. Devereaux, D. Einzel, B. Stadlober, R. Hackl, D. H. Leach, and J. J. Neumeier, Phys. Rev. Lett. **72**, 396 (1994).

[13] D. A. Wollman, D. J. Van Harlingen, W. C. Lee, D. M. Ginsberg, and A. Leggett, Phys. Rev. Lett. **71**, 2134 (1993).

[14] A. G. Sun, D. A. Gajewski, M. B. Maple, and R. C. Dynes, Phys. Rev. Lett. **72**, 2267 (1994).

[15] C. C. Tsuei, J. R. Kirtley, C. C. Chi, L. S. Yu-Jahnes, A. Gupta, T. Shaw, J. Z. Sun, and M. B. Ketchen, Phys. Rev. Lett. **73**, 593 (1994).

[16] D. A. Brawner and H. R. Ott, Phys. Rev. B **50**, 6530 (1994).

[17] A. Mathai, Y. Gim, R.C. Black, A. Amar, and F.C. Wellstood, Phys. Rev. Lett. **74**, 4523 (1995).

[18] J. Annett, N. Goldenfeld, and S. R. Renn, Phys. Rev. B **43**, 2778 (1991).

[19] A. Junod, in *Physical Properties of HTSC II*, edited by D. Ginsberg (World Scientific, Singapore, 1990).

[20] N. E. Phillips, R. A. Fisher, and J. E. Gordon, in *Progress in Low Temperature Physics*, edited by D. F. Brewer (Elsevier Science Publishers B. V., Amsterdam, 1992), Vol. 13, pp. 267–357.

[21] J. W. Loram, K. A. Mirza, J. R. Cooper, and W. Y. Liang, Phys. Rev. Lett. **71**, 1740 (1993).

[22] M. Prohammer, A. Perez-Gonzalez, and J. P. Carbotte, Phys. Rev. B **47**, 15 152 (1993).

[23] D. Scalapino (private communication).

[24] R. B. Laughlin (private communication).

[25] K. A. Moler, Ph.D. thesis, Stanford University, 1995.

[26] G. E. Volovik, JETP Lett. **58**, 469 (1993).

[27] R. Bachmann, F. J. DiSalvo, Jr., T. H. Geballe, R. L. Greene, R. E. Howard, C. N. King, H. C. Kirsch, K. N. Lee, R. E. Schwall, H.-U. Thomas, and R. B. Zubeck, Rev. Sci. Instrum. **43**, 205 (1972).

[28] F. Hellman, Ph.D. thesis, Stanford University, 1985.

[29] S. R. Early, Ph.D. thesis, Stanford University, 1981; J. S. Urbach, Ph.D. thesis, Stanford University, 1993.

[30] Ruixing Liang, P. Dosanjh, D. A. Bonn, D. J. Baar, J. F. Carolan, and W. N. Hardy, Physica C **195**, 51 (1992).

[31] A. P. Ramirez, R. J. Cava, G. P. Espinosa, edited by M. B. Brodsky, R. C. Dynes, K. Kitazawa, H. L. Tuller, J. P. Remeika, B. Batlogg, S. Zahurak, and E. A. Reitman, in *High-Temperature Superconductors*, MRS Symposia Proceedings No. 99 (Materials Research Society, Pittsburgh, 1987), p. 459.

[32] N. W. Ashcroft and N. D. Mermin, *Solid State Physics* (W. B. Saunders Company, Philadelphia, 1976).

[33] V. V. Chabanenko, I. B. Krynetskii, S. Piechota, and H. Szymczak, Physica B **289-290**, 216 (1996).

[34] P. Lemmens, P. Fröning, S. Ewert, J. Pankert, H. Passing, and A. Comberg, Physica B **165-166**, 1275 (1990).

[35] D. Sanchez, A. Junod, J.-Y. Genoud, T. Graf, and J. Muller, Physica C **200**, 1 (1992).

[36] T. E. Mason, G. Aeppli, S. M. Hayden, A. P. Ramirez, and H. A. Mook, Phys. Rev. Lett. **71**, 919 (1993).

[37] J. P. Emerson, R. A. Fisher, N. E. Phillips, D. A. Wright, and E. M. McCarron III, Phys. Rev. B **49**, 9256 (1994).

[38] R. A. Fisher, J. E. Gordon, S. F. Reklis, D. A. Wright, J. P. Emerson, B. F. Woodfield, E. M. McCarron III, and N. E. Phillips, Physica C **252**, 237 (1995).

[39] C. Caroli, P. G. deGennes, and J. Matricon, Phys. Lett. **9**, 307 (1964).

[40] A. L. Fetter and P. Hohenberg, in *Superconductivity*, edited by R. D. Parks (Marcel Dekker, Inc., New York, 1969), Vol. 2, pp. 817–923.

[41] R. Radebaugh and P. H. Keesom, Phys. Rev. **149**, 209 (1966).

[42] L. N. Bulaevskii and M. P. Maley, Phys. Rev. Lett. **71**, 3541 (1993); and (private communication).
[43] A. L. Fetter, Phys. Rev. B **50**, 13 695 (1994).
[44] K. A. Moler, A. L. Fetter, and A. Kapitulnik, J. Low Temp. Phys. **100**, 185 (1995).
[45] G. R. Stewart and B. L. Brandt, Phys. Rev. B **29**, 3908 (1984).
[46] A. Ramirez, Phys. Lett. A **211**, 59 (1996).
[47] K. Karrai, E. J. Choi, F. Dunmore, S. Liu, H. D. Drew, Qi Li, D. B. Fenner, Y.D. Zhu, and Fu-Chun Zhang, Phys. Rev. Lett. **69**, 152 (1992).
[48] I. Maggio-Aprile, Ch. Renner, A. Erb, E. Walker, and O Fischer, Phys. Rev. Lett. **75**, 2754 (1995).
[49] P. I. Soininen, C. Kallin, and A. J. Berlinsky, Phys. Rev. B **50**, 13 883 (1994).
[50] N. Schopohl and K. Maki (unpublished).
[51] A. J. Berlinsky, A. L. Fetter, M. Franz, C. Kallin, and P. I. Soininen, Phys. Rev. Lett. **75**, 2200 (1995).
[52] B. Efron, *An Introduction to the Bootstrap* (Chapman and Hall, New York, 1993).
[53] Y. Nakazawa and M. Ishikawa, Physica C **162-164**, 83 (1989).
[54] B. Parks, S. Spielman, J. Orenstein, D. T. Nemeth, F. Ludwig, J. Clarke, P. Merchant, and D. J. Lew, Phys. Rev. Lett. **74**, 3265 (1995).
[55] G. E. Volovik (unpublished).
[56] D. S. Dessau, Z.-X. Shen, D. M. King, D. S. Marshall, L. W. Lombardo, P. H. Dickinson, A. G. Loeser, J. DiCarlo, C.-H. Park, A. Kapitulnik, and W. E. Spicer, Phys. Rev. Lett. **71**, 2781 (1993).
[57] N. Momono, M. Ido, T. Nakano, M. Oda, Y. Okajima, and K. Yamaya, Physica C **233**, 395 (1994).
[58] A. Ramirez, N. Stucheli, and E. Bucher, Phys. Rev. Lett. **74**, 1218 (1995).
[59] C. M. Varma (private communication).
[60] P. J. Hirschfeld and N. Goldenfeld, Phys. Rev. B **48**, 4219 (1993).
[61] P. J. Hirschfeld, W. O. Putikka, and D. J. Scalapino, Phys. Rev. B **50**, 10 250 (1994).